Spatial Variability of Input Motion in Stochastic Slope Stability

Pooneh Shah Malekpoor[1](✉), Susana Lopez-Querol[1], and Sina Javankhoshdel[2]

[1] University College London (UCL), London WC1E 6BT, UK
pooneh.shahmalekpoor.19@ucl.ac.uk
[2] Rocscience, Inc., 54 St. Patrick St., Toronto, ON M5T 1V1, Canada

Abstract. The slope stability has been widely analysed in the past, which demonstrates the significance of the subject in human life, especially in terms of life safety and economy. This is even more important in earthquake-prone areas where statically stable slopes may be triggered by the dynamic loads. Pseudo-static (PS) approaches are most used in the first stages of the regular assessment of seismic slope stability analysis. However, the spatial variability of the PS coefficient has not been considered so far in the realm of PS analyses, meaning that the value of the seismic coefficient is assumed to be constant at every location within a field while this is not true in the real case. The consideration of the variation of the PS coefficient is especially relevant to landslides in wide areas. This research aims at addressing this issue considering the stochastic nature of soils in seismic slope stability analysis within the framework of the limit equilibrium method (LEM) of slices, Monte Carlo (MC) simulation and random fields, termed 2D-RLEM. Results of parametric studies are presented, through which the sensitivity of stochastic slope stability problem to various factors, including different levels of spatially variable PS loading, the scale of fluctuation (SOF) of the PS coefficient random field, etc, are explored. It was concluded that the effect of different values assigned to the coefficient of variation and the SOF of the PS coefficient on the resulting slope probabilities of failure was more tangible for larger earthquakes.

Keywords: Slope Stability · Seismic Slope Stability · PS Approach · Soil Spatial Variability · Spatial Variability of Input Load

1 Introduction

The stability of slopes is of high significance due to their utility in terms of being near, or part of, large engineered structures, such as bridges and dams. To speed up the slope stability analyses in seismic-prone areas, simplified equivalent-seismic procedures (i.e. pseudo-static (PS) approach) are commonly used compared to other methodologies including more rigorous dynamic analyses that entail detailed-modelling as well as considerable computation time (Baker et al., 2006; Burgess et al., 2019). A PS approach is mainly based on a horizontal PS coefficient (K_h) the values of which have been suggested by previous studies (Melo and Sharma, 2004; Jibson, 2011) while the effect of the vertical component is recognised as less significant (Gazetas et al. 2009; Zhang

S. Javankhoshdel and Y. Abolfazlzadeh (Eds.): TMIC 2022, AHE 13, pp. 179–198, 2023.
https://doi.org/10.2991/978-94-6463-104-3_17

et al. 2015). According to Baker (2021), the seismic intensity measure (IM) that each structure (that can be interpreted as distinct locations in sloped areas) experiences when dealing with spatially distributed systems (e.g. slopes) is different due to the differing distances from each considered earthquake rupture to the locations of interest, differing site conditions at each location, and other effects such as rupture heterogeneity, wave propagation and scattering. However, the simplified PS approach merely considers a constant value as the seismic load.

Soil properties (e.g. cohesion and friction angle) are stochastic as well due to different deposition conditions and loading histories in an area (Elkateb et al., 2003). Indeed, such a spatially variable nature would have a significant effect on the results of geotechnical reliability analyses if reflected correctly in mathematical models as it helps to simulate a more realistic picture of the soil structure.

With regards to these stochastic features, a new methodology has been developed and presented in this paper, to consider these factors simultaneously and make the simulations more realistic as well as time-efficient for a seismic geotechnical problem.

2 Literature Review

2.1 Pseudo-static Approach

In the PS approach, a horizontal force (K_h*W), where K_h is the PS coefficient and W is the weight of the sliding mass of soil slope, is applied to the centre of the gravity (COG) of a sliding mass (or COG of each slice in limit equilibrium of slices (LEM of slices) instead of the real complex seismic load (Mostyn and Small, 1987). According to Leshchinsky and San (1994) and Baker et al. (2006), the PS coefficient depends on the seismological features, including earthquake magnitude and focal distance. Table 1 represents a summary of PS coefficient values from previous studies.

Several researchers have developed PS slope stability design charts for simple homogeneous slopes based on the PS approach used within the framework of either limit analysis, limit equilibrium or finite elements (Koppula, 1984; Leshchinsky and San, 1994; Michalowski, 2002; Loukidis et al., 2003; Baker et al., 2006; Burgess et al., 2019). Depending on the charts' format, the critical horizontal seismic coefficient (K_{hc}) (corresponding to a PS factor of safety (F_{PS}) equal to 1) or F_{PS} for a given PS coefficient can be obtained (Leshchinsky and San, 1994; Burgess et al., 2019). More specifically, the PS approach has been widely used within the LEMs (Baker et al., 2006; Park et al., 2018). In the PS-LEM of slices (e.g. Loukidis et al., 2003; Choudhury et al., 2007), the inertial force K_h*W_i (W_i being the slice weight) is inserted into the equations of static equilibrium and applied at the COG of each slice. The output would be the PS factor of safety, which is expected to decrease as the seismic load increases.

2.2 Spatial Variability

Different depositional conditions and stress histories in a sloped area, as well as variations in the mineralogical composition, are some of the factors causing soil properties to vary from one location to another, being known as the soil inherent variability. This

Table 1. PS coefficients from different studies (Jibson, 2011)

Reference	Recommended PS coefficient (K_h)	Recommended factor of safety	Calibration conditions
Terzaghi (1950)	0.1(R-F = IX)[a] 0.2(R-F = X) 0.5(R-F > X)	>1.0	Unspecified
Seed (1979)	0.10(M = 6.50)[b] 0.15(M = 8.25)	>1.15	<1 m displacement in earth dams
Marcusen (1981)	(0.33 – 0.50)*PGA[c]/g	>1.0	Unspecified
Hynes-Griffin and Franklin (1984)	0.50*PGA/g	>1.0	<1 m displacement in earth dams
California Division of Mines and Geology (1997)	0.15	>1.1	Unspecified; probably based on <1 m displacement in dams

[a] R-F is the Rossi-Forel earthquake intensity scale.
[b] M is earthquake magnitude.
[c] PGA is the peak ground acceleration.

has been the main subject of research by Phoon et al. (1995) and Phoon and Kulhawy (1999a) who reported a very comprehensive literature review study, as well as tabular and graphical presentations for the coefficient of variation (COV) of the inherent variability of different soil parameters, classified based on the soil and test types. Other sources of uncertainty and variability in soil data are attributed to measurement errors and transformation uncertainty (Phoon and Kulhawy, 1999a, 1999b). Only the inherent variability of the soil properties can be modelled through the theory of random fields (Sasanian et al., 2021). Vanmarcke's random field theory is commonly implemented to model this inherent spatial variability within an area (Vanmarcke, 1988). The least number of inputs are required to generate a stationary Gaussian random field including the mean of the soil property, COV of inherent variability component, type of the probabilistic distribution of soil data (normal, lognormal), and the correlation model between the inherent variability components. These values can be obtained from several available studies (Phoon et al., 1995; Phoon and Kulhawy, 1999a; Duncan, 2000; Cherubini, 2000; Wu, 2013; Cami et al., 2020; ISSMGE-TC304, 2021). For example, Phoon and Kulhawy (1999a) presented ranges of COV values for soil friction angle and cohesion, (COV_ϕ and COV_c), respectively reported as (5–15)% and (10–55)%. For this range of COV_ϕ, Phoon and Kulhawy (1999a) presented a range of mean values (μ_ϕ) between 20º and 40º. Regarding the mean undrained cohesion value (μ_c), a range of 10–700 kPa was recommended (Phoon and Kulhawy, 1999a). The Markovian autocorrelation function (ACF) for a two-dimensional (2D) Gaussian random field is defined as

$$\rho(\Delta_H, \Delta_V) = exp\left\{-\sqrt{\left(\frac{2\delta_H}{\theta_H}\right)^2 + \left(\frac{2\delta_V}{\theta_V}\right)^2}\right\} = \exp\left\{-\frac{2\delta}{\theta}\right\} \quad (1)$$

where δ_H and δ_V are the absolute horizontal and vertical distances between two locations within the random field and θ_H and θ_V are the scales of fluctuation (SOFs) in the horizontal and vertical directions, respectively, with $\delta = \sqrt{(\delta_H{}^2 + \delta_H{}^2)}$ and θ being the isotropic SOF for a 2D isotropic Gaussian random field (Burgess et al., 2019; Cami et al., 2020). The SOF is expressed as the distance within which the soil property is highly correlated and is calculated as the area under the correlation function or estimated via different procedures such as the Method of Moments (MOM), Maximum-likelihood (MLE) and Bayesian analysis from limited soil sample data (El-Ramly, 2001; Cami et al., 2020). Cami et al. (2020) provided a summary of scales of fluctuation of different soils from the literature.

Various random-field generator algorithms are available to produce stochastic models, the most common of which are: Moving-average (MA) method, Discrete Fourier transform (DFT) method, Covariance matrix decomposition (CMD), Fast Fourier Transform (FFT) method, Turning-bands method (TBM) and Local average subdivision (LAS) method (Fenton and Griffiths, 2008). Among them, the most widely-used are CMD and LAS considering that FFT, TBM, and LAS methods are typically much more efficient than the other ones. If the problem at hand requires, or benefits from, a local average representation (e.g. soil statistical modelling), then the LAS method is the logical choice, though other generators are also commonly-used (Fenton and Griffiths, 2008; Huang et al., 2013; Jamshidi Chenari and Alaie, 2015).

Different studies have considered the soil spatial variability in slope reliability analysis (Griffiths and Fenton, 2004; Srivastava and Babu, 2009; Griffiths et al., 2009; Huang et al., 2010; Huang et al., 2013; Li et al., 2014; Jamshidi Chenari and Alaie, 2015; Cami et al., 2017; Javankhoshdel et al., 2017; Burgess et al., 2019). Griffiths and Fenton (2004) employed the random finite element method (RFEM), which is a combination of the random field theory (i.e. using LAS), Monte Carlo (MC) simulation and finite element method (FEM) for the reliability analysis of a purely cohesive slope and concluded that the perfect correlation assumption leads to unconservative results for slopes with low factor of safety or when the soil COV is relatively high. One of the important features of the RFEM is that it allows the failure mechanism to naturally seek out the weakest failure path (Griffiths and Fenton, 2004). Srivastava and Babu (2009) investigated the effect of the soil spatial variability on the reliability of a cohesive-frictional slope. Based on the static cone penetration test (SCPT) data and considering the autocorrelation function versus lag graph, they found out that the corresponding inherent variability components were uncorrelated and thus only the depth-variable trend was considered.

Griffiths et al. (2009) compared the resulting probability of slope failure from FEM, combined with a first-order reliability method (FORM) without spatial variation, with a more advanced RFEM approach and found a critical value for COV of the soil shear strength parameters at which the single random variable (SRV) approach, which assumes a perfect correlation condition, becomes unconservative. Along the same vein, Huang et al. (2010), concluded that RFEM is more reliable as it can accurately predict the system probability of failure of slopes rather than the probability of failure of the most critical slip surface (corresponding to higher reliability compared to the system reliability) as it is in FORM (no spatial variability). By employing Karhunen-Loeve expansion method for modelling the stochastic purely cohesive soil applied to some theoretical slopes, Huang

et al. (2013) proposed a new framework for quantitative risk assessment of landslides, based on the logic that the consequence should be assessed individually for each failure mode. Li et al. (2014) adopted a nonstationary random field model to investigate the effect of the soil spatial variability on the stability of clay as well as sandy infinite slopes. With the use of stationary and non-stationary random fields generated from CMD method, Jamshidi Chenari and Alaie (2015) investigated the effect of the anisotropic spatial variation in the undrained shear strength on the reliability of clay slopes through a RFDM approach (Random Finite Difference method). Burgess et al. (2019) developed the first so-called seismic probabilistic slope stability design aids by adopting the PS approach and considering the cohesive-frictional soil spatial variability within the RFEM approach. However, the superiority of RFEM has been arguably outshined by the massive computational effort embedded in the strength reduction technique (Javankhoshdel et al., 2017; Cami et al., 2017).

The random limit equilibrium method (RLEM) was first introduced and utilized by Javankhoshdel et al. (2017), being a combination of circular LEM, random field theory and MC simulation where stochastic values are generated using the LAS method by Fenton and Vanmarcke (1990) and mapped onto a grid of elements (mesh); each element of the grid is assigned a random value which correlates with the nearby values based on a correlation length. The RLEM has been used extensively to interpret the uncertainty embedded in the slope stability analyses assuming both circular and non-circular slip surfaces (Cami et al. 2017). Javankhoshdel and Bathurst (2014) and Javankhoshdel et al. (2017) utilized circular-RLEM to investigate the influence of soil spatial variability on the slope probability of failure. Lately, the advent of the new search and optimization techniques like Cuckoo search and Surface Altering Optimization (SAO) (as discussed in Shah Malekpoor et al., 2020), promoted to seeking for non-circular failure surfaces (Tabarroki et al., 2013; Javankhoshdel et al., 2018; Cami et al., 2017; Shah Malekpoor et al., 2020).

Regarding the dynamic input loads, it is worth noting that real earthquakes vary spatially according to three effects: wave passage effect (the difference in the arrival time of a seismic load in different areas), incoherence effect (due to the reflection and refraction of seismic excitations), and local soil effect (where amplitude and frequency content of an input load changes due to the local site effects) (Saxena et al., 2000). However, the simplistic PS approach does not take such effects into account. The stochastic nature of the real seismic loads can be, instead, simulated roughly by considering a stochastic nature for the seismic coefficient in a PS approach within the area under investigation. For the PS coefficient, Tsompanakis et al. (2010) assumed a lognormal distribution with a mean value (μ_{Kh}) in the range of (0.01–0.5) g and COV_{Kh} of 10%. Youssef Abdel Massih et al. (2008) explored the effect of two distributions: exponential distribution (Exp D) and an extreme value type II distribution (EVD) for the PS coefficient with a COV in the range of (10–80)%. Notwithstanding, no spatial variation has ever been considered for the PS coefficient. Hence, the current research aims at implementing the spatial variability of the PS coefficient and exploring its effects on different aspects of stochastic slope stability analysis.

3 Methodology

The models presented in this paper are simple homogeneous slopes (i.e. single material) made up of cohesive-frictional soils. The complex geometries are not considered as the goal is to focus on the effect of the spatial variability of K_h. Random fields for soil properties and PS coefficient are considered isotropic stationary Gaussian (Fenton and Griffiths, 2008) with lognormal distribution due to their nonnegative nature based on literature studies (Javankhoshdel et al., 2017). No cross-correlation has been considered between the random variables. It should be noted that the given soil slope is considered as dry and the effect of pore pressure on the stability is not taken into consideration for the current stage of this research but will be also considered in the future. Figure 1 shows the sample slope analysed in this study.

According to Cami et al. (2020), the SOF of mixed c-ϕ soil is taken here as $\delta_H = 200$ m and $\delta_V = 1.5$ m with a Markovian ACF. Though the statistical features for the PS coefficient were chosen similar to Tsompanakis et al. (2010) (i.e. a lognormal distribution with a mean value in the range of (0.01–0.5), a range of COV (i.e. 0.1, 0.3, 0.5) was employed to explore the effect of different variability levels of seismic load within the field.

In summary, the deterministic and statistical parameter values of simulations have been presented in Table 2 (Phoon and Kulhawy, 1999a; Melo and Sharma, 2004; Jibson, 2011; Burgess et al., 2019; Cami et al., 2020).

As in the reliability analysis technique, MC simulations have been used, consisting of a number of limit equilibrium analyses of the slope (in each iteration). For each MC iteration, 5000 realizations in total, i.e. samples of random field variables, were generated with the *mrslope2d* code by Fenton and Griffiths (2008) (inputting the mean, standard deviation, mesh size, SOF, type of probabilistic distribution and ACF) and imported as the inputs to the authors' developed code in MatLab R2021b. This approach is called 2D-RLEM as stated in the literature (Javankhoshdel et al. 2017). The mesh size is recommended to be less than half of the SOF (Huang and Griffiths, 2015), e.g. being 0.5*0.5 when SOF = 1.5 m. In fact, the slope section is divided into grids (elements) and the imported random values (for each random variable; c, ϕ and K_h) from *mrslope2d* are assigned to each element. Implementing the LEM of slices, each slice base is located

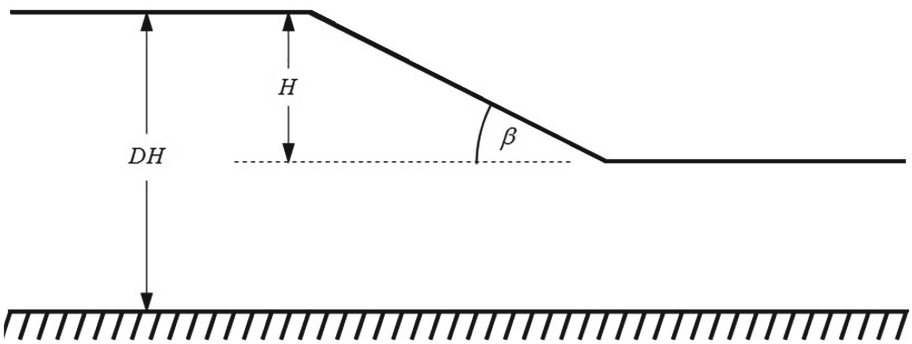

Fig. 1. Sample slope section

Table 2. List of simulation parameters

Parameter	Values considered
β, Slope angle	20º to 85º
μ_ϕ	20º, 25º, 30º
Stability number, $\lambda = \mu_c / \gamma H tan \mu_\phi$	0.1, 0.2, 0.3, 0.4, 0.5, 0.6, 0.7, 0.8
μ_c	Determined based on λ
μ_{Kh}	0.1, 0.3, 0.5
COV_c	0.3
COV_ϕ	0.15
COV_{Kh}	0.1, 0.3, 0.5
Unit weight of soil, γ	18 (kN/m^3)
Slope height, H	5 m
Depth factor, D[a]	2
$(\theta_{c,\phi})_{Ho}$[b]$/H$	40
$(\theta_{c,\phi})_V$[c]$/H$	0.3
$\theta_{Kh(H,V)}$[d]$/H$	0.3, 1, 2, 5, 200

[a] The depth factor is simply taken as the depth to the hard layer divided by the height of the slope
[b] Horizontal SOF of soil
[c] Vertical SOF of soil
[d] Isotropic SOF of the PS coefficient

within an element, the assigned value of which will be adopted as the random value of that property (cohesion, friction angle or PS coefficient random values) for the whole slice (Javankhoshdel and Bathurst, 2014). Then, the PS safety factor of each slip surface is calculated with the Bishop simplified method in each MC iteration. This method is chosen among different LEM of slices due to its efficiency and accuracy investigated by the authors and also asserted in the literature (Fredlund and Krahn, 1977). At the end of each iteration (and exploring the PS safety factor of different slip surfaces), the PS safety factor of the critical slip surface (the one with the minimum Bishop PS factor of safety) is compared to unity. The slope probability of failure is finally calculated as the number of iterations with a PS factor of safety less than one with respect to the total number of iterations (Shah Malekpoor and Lopez-Querol, 2022).

To find the optimal number of MC iterations, 2D-RLEM analyses were run for different numbers of samples preceding the main parametric studies. The optimal sample number is the one for which the probability of failure versus the number of samples graph starts getting a stable value. This was conducted for a number of cases. It was observed that 20,000 samples were enough for small probabilities of failure (i.e. (0–0.1) %) as the plot in Fig. 2 starts to stabilize from 20,000 samples (highly variable as well as unreliable probabilities before that), while 5000 samples were sufficient for higher probabilities of failure (i.e. (0.1–100)%) based on the sample convergence plot (Fig. 3).

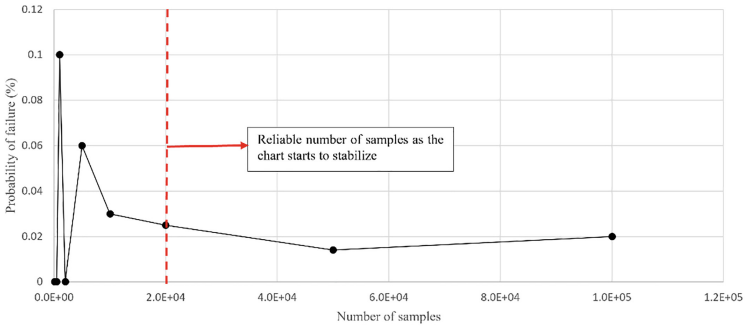

Fig. 2. Optimal number of MC samples for probabilities of failure in the range (0–0.1)% (for the case: $\beta = 60°$, $\mu_\phi = 20^{\circ}$, $\lambda = 0.6$, $\mu_{Kh} = 0.1$, $H = 5$ m, $\gamma = 18$ kN/m^3, $\mathrm{COV}_c = 0.3$, $\mathrm{COV}_\phi = 0.15$, $\mathrm{COV}_{Kh} = 0.5$, $(\theta_{c,\phi})_{Ho}/H = 40$, $(\theta_{c,\phi})_V/H = 0.3$, $\theta_{Kh(H,V)}/H = 0.3$

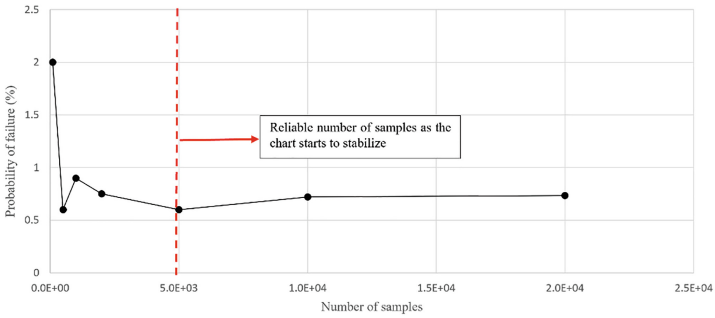

Fig. 3. Optimal number of MC samples for probabilities of failure in the range (0.1–100)% (for the case: $\beta = 70°$, $\mu_\phi = 20^{\circ}$, $\lambda = 0.6$, $\mu_{Kh} = 0.1$, $H = 5$ m, $\gamma = 18$ kN/m^3, $\mathrm{COV}_c = 0.3$, $\mathrm{COV}_\phi = 0.15$, $\mathrm{COV}_{Kh} = 0.5$, $(\theta_{c,\phi})_{Ho}/H = 40$, $(\theta_{c,\phi})_V/H = 0.3$, $\theta_{Kh(H,V)}/H = 0.3$

4 Results

This novel methodology is expected to result in the first series of seismic stochastic slope stability design aids showing the effect of different intensities of spatially variable PS coefficient on the probability of failure of stochastic soil slopes. In fact, they could be an improvement form of Burgess et al. (2019) charts, for which a constant value was considered for the PS coefficient. However, the current preliminary research focuses on the results of some parametric studies including the sensitivity of the theoretical stochastic slope stability problem to factors including (but not limited to) various levels of spatially variable PS coefficient, different degrees of COV_{Kh}, the value of the SOF of the PS coefficient, and the friction angle of soil material. It is worth noting that the solid lines in Figs. 4, 5, and 6 represent the deterministic factor of safety values for different slope angles and stability numbers while the dashed lines correspond to probability of failure value both under three different levels of PS coefficient mean value. For example, the red arrow (pointing to the right) in Fig. 5 shows the PS factor of safety of a slope with $\beta = 40°$, $\lambda = 0.6$, $\phi = 20°$, and $K_h = 0.3$ (deterministic parameter values) is 1.39.

On the other hand, the probability of failure for this slope in a spatially variable context with statistical parameters mentioned in the caption of the corresponding figure is shown by another red arrow (pointing to the left) and is estimated to be 2.16% when COV_{Kh} is 0.5.

4.1 The Effect of μ_{Kh}, COV_{Kh} and λ

The first parametric study was dedicated to exploring the effect of different levels of magnitude for the spatially variable PS coefficient in a stochastic slope stability problem considering different levels of variability within the PS random field and different stability numbers, λ. In this regard, three values were inputted as μ_{Kh} values e.g. 0.1, 0.3, and 0.5 for various levels of COV_{Kh} e.g. 0.1, 0.3 and 0.5, standardized SOF of 0.3 for the PS generated random field and different stability numbers which led to different levels of failure (parameters described in Table 2 and results in Figs. 4, 5, and 6).

As is expected, a higher stability number (i.e. a higher cohesive strength when the slope height and friction angle are constant) results in a lower probability of failure for a particular slope angle subjected to a spatially variable PS loading while a higher mean magnitude for the PS coefficient yields higher risk of failure for a specific slope.

Regarding a specific amount of failure probability, increases in stability factor from left to right, shifts the graphs to higher slope angles.

It was observed in Fig. 4 that there is quite no difference between the results considering different COV_{Kh} values for a low amount of stochastic PS loading (i.e. 0.1). However, Figs. 5 and 6 show that the higher the amount of the stochastic PS loading, the more tangible is the effect of the level of variation, COV, in the PS coefficient within the field. In other words, the effect of different COV_{Kh} values, of PS load is critical to be considered especially for large magnitude earthquakes, the equivalent PS coefficient of which is higher (according to Table 1).

As the mean value of the seismic coefficient increases to 0.3, a turning point starts to emerge in charts that shows a higher COV_{Kh} (i.e. 0.5) in PS coefficient results in greater vulnerability for a specific slope angle except for very high probabilities of failure (i.e. more than 50% for $\lambda = 0.6$ in Fig. 5) where a low COV_{Kh} value is more critical. This turning point shifts to lower probabilities of failure and higher slope angles for greater stability factors (from left to right in Fig. 5) till it becomes disappeared for $\mu_{Kh} = 0.5$ when $\lambda = 0.8$ (Fig. 6). In fact, a COV_{Kh} of 0.5 is observed to be the critical value for a mean PS coefficient value of 0.5 as it results in the highest risk of failure for almost all the slope angles except for very high probability of failure values (i.e. more than 90%) (Fig. 6).

Meanwhile, a lower level of variation for the PS coefficient (in charts with higher μ_{Kh} where the distinction between COV graphs becomes obvious) leads to a steeper change in the charts slope (Figs. 5 and 6). In fact, the rate at which the risk of slope failure increases with an increase in the slope inclination is higher for a smaller COV_{Kh} value.

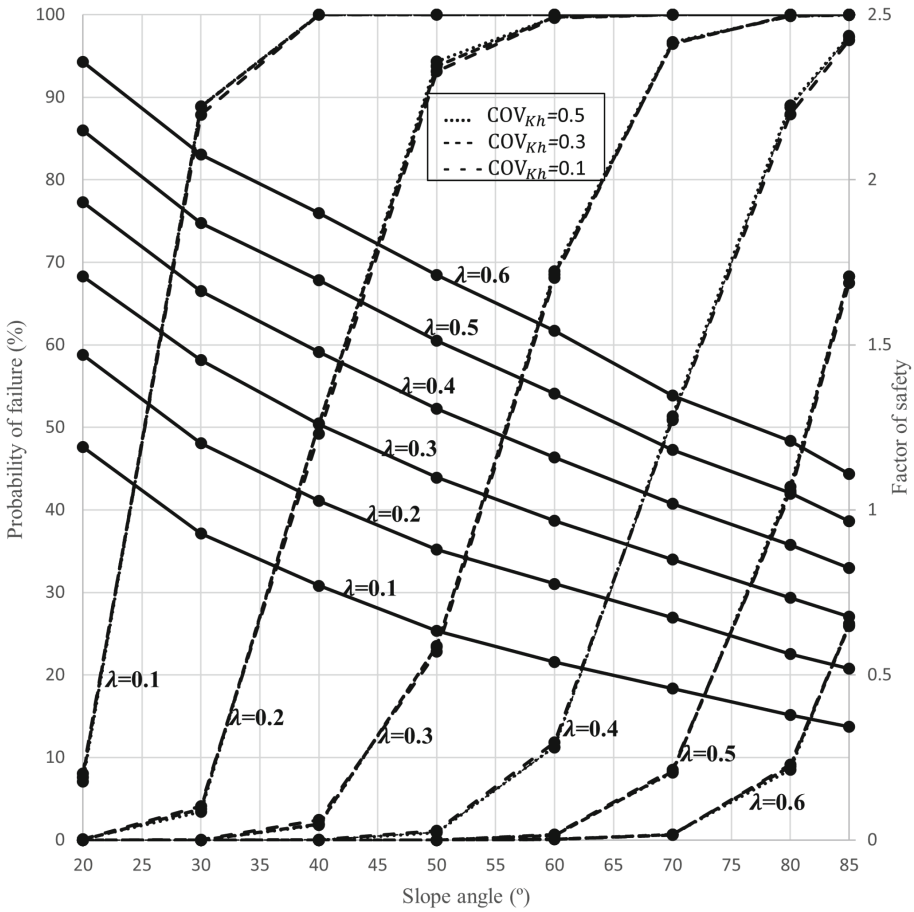

Fig. 4. The effect of various levels of COV$_{Kh}$ and λ for $\mu_{Kh} = 0.1$, $\mu_{\phi} = 20^{\circ}$, COV$_c = 0.3$, COV$_{\phi} = 0.15$, $(\theta_{c,\phi})_{Ho}/H = 40$, $(\theta_{c,\phi})_V/H = 0.3$, $\theta_{Kh(H,V)}/H = 0.3$ with a Markovian ACF

4.2 The Effect of θ_{Kh}

The novelty of the current research is associated with the inclusion of the spatial variability of the PS coefficient (θ_{Kh}) within a stochastic slope stability problem. This effect has been explored through parametric studies over a number of SOF values for different mean values of the PS coefficient (0.1, 0.3 and 0.5) considering a stochastic slope.

The same as the ineffectiveness of the COV$_{Kh}$ in low mean values of PS coefficient, different θ_{Kh} values do not affect the resulting probabilities of failure of a slope (with the same soil material but different angles) subjected to a small mean PS coefficient value of 0.1 (Fig. 7).

For higher mean values of PS coefficient (i.e. 0.3 and 0.5), it was observed that the more non-smooth is the random field for the PS coefficient (i.e. the smaller is the SOF value for the PS coefficient random field), the higher is the risk of failure for all slope angles when the probability of failure is very high (Figs. 8 and 9). The small SOF

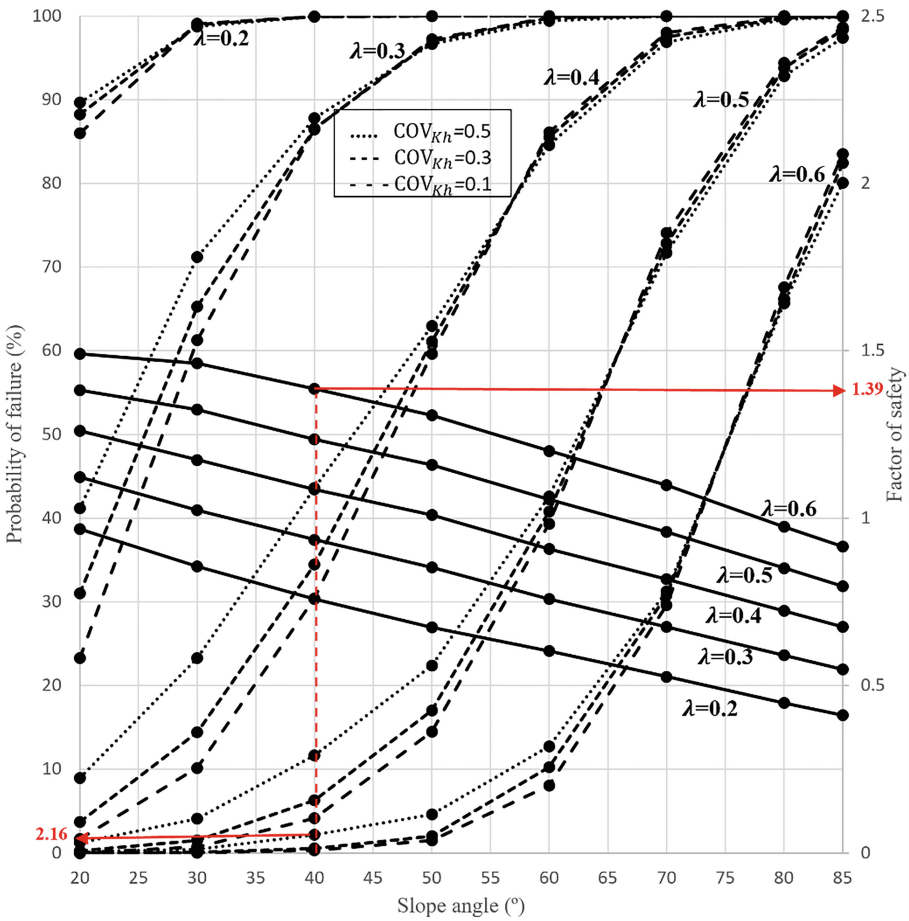

Fig. 5. The effect of various levels of COV_{Kh} and λ for $\mu_{Kh} = 0.3$, $\mu_{\phi} = 20^{\circ}$, $COV_c = 0.3$, $COV_{\phi} = 0.15$, $(\theta_{c,\phi})_{Ho}/H = 40$, $(\theta_{c,\phi})_V/H = 0.3$, $\theta_{Kh(H,V)}/H = 0.3$ with a Markovian ACF

value (i.e. 1.5 m) corresponding to the highest probabilities of failure is interpreted as the worst-case SOF value which is of high importance in conservative and safe slope designs (Figs. 8 and 9). The only discrepancy in the trend is with respect to SOF = 1.5 m for slope angles less than 50º and μ_{Kh} equal to 0.3 (Fig. 8). This SOF value yields the smallest probability of failure for slope angles less that about 35º in Fig. 8. According to Fig. 9, a big difference between the resulting probabilities of failure for considering the spatial variability of the PS coefficient and disregarding this effect was observed for a large earthquake with $\mu_{Kh} = 0.5$ for gentle slopes (i.e. 20º and 30º).

All the Figs. of 7, 8 and 9 follow a logical trend that a steeper slope angle leads to a higher risk of failure for all SOF values of the PS coefficient and a higher probability of failure arises from a greater mean value for the PS coefficient for all slope angles.

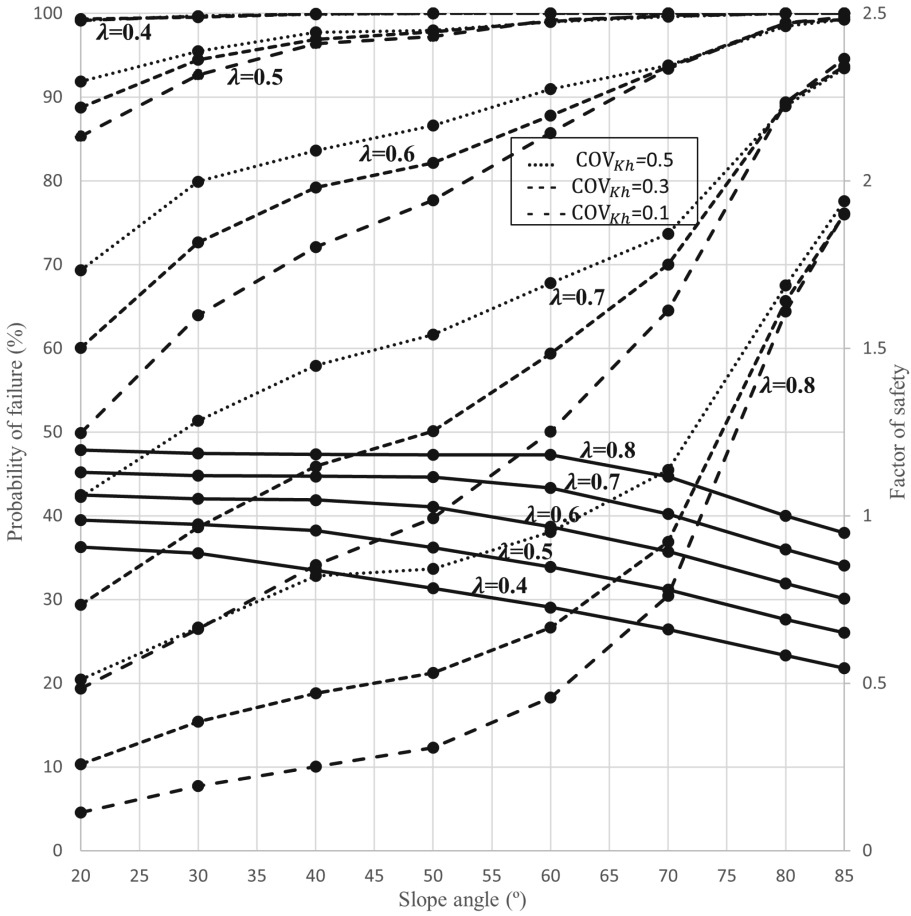

Fig. 6. The effect of various levels of COV_{Kh} and λ for $\mu_{Kh} = 0.5$, $\mu_{\phi} = 20^{\circ}$, $COV_c = 0.3$, $COV_{\phi} = 0.15$, $(\theta_{c,\phi})_{Ho}/H = 40$, $(\theta_{c,\phi})_V/H = 0.3$, $\theta_{Kh(H,V)}/H = 0.3$ with a Markovian ACF

4.3 The Effect of μ_{ϕ}

The effect of soil friction angle and its relationship with the spatial variability of the PS coefficient has been explored and the outputs are presented here. According to the results in Fig. 10, a higher mean value for the friction angle results in a lower risk of failure for a specific slope angle when all the other parameters are the same (as expected). Small differences exist between the resulting probabilities of failure for a higher mean value for the friction angle (for a constant λ) under different values of COV_{Kh} in a specific slope especially for more gentle slope angles when $\theta_{Kh(H,V)}/H = 0.3$ (e.g. 20º–40º). Meanwhile, higher COV_{Kh} values lead to a higher probability of failure except for high risks of failure for both mean values of friction angle.

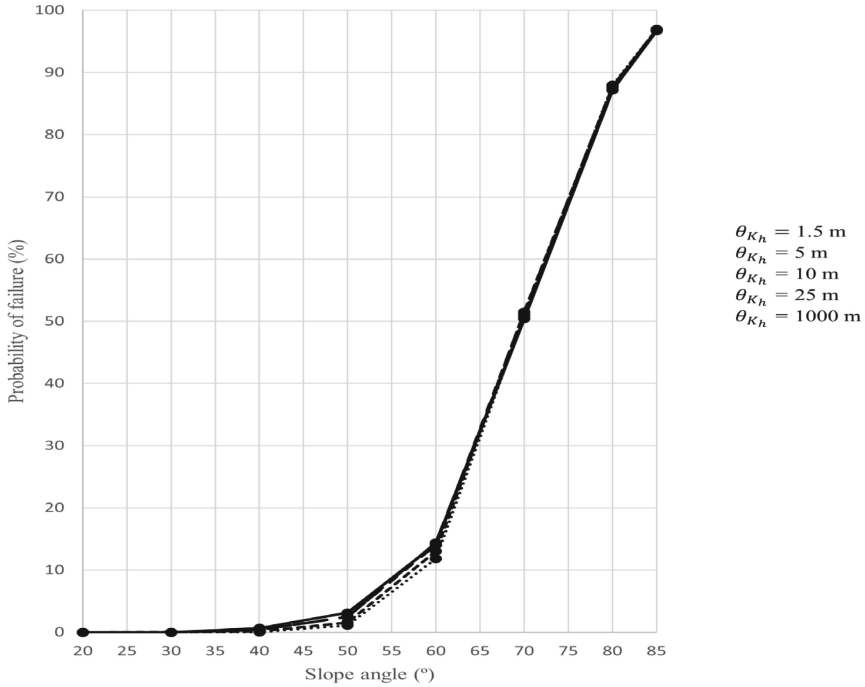

Fig. 7. The influence of θ_{Kh} on probability of slope failure for $\mu_{Kh} = 0.1$, $\mu_\phi = 20^\circ$, $\lambda = 0.4$, $\mathrm{COV}_c = 0.3$, $\mathrm{COV}_\phi = 0.15$, $\mathrm{COV}_{Kh} = 0.5$, $(\theta_{c,\phi})_{Ho}/H = 40$, $(\theta_{c,\phi})_V/H = 0.3$, $\theta_{Kh(H,V)}/H = 0.3$ with a Markovian ACF

Based on Fig. 11, the perfect correlation case (when SOF value is 1000 m) is the worst-case SOF for slope angles up to 60º while the smallest SOF value takes that role for steeper slope angles. For a higher mean friction angle in Fig. 12, the perfect correlation case yields the highest probabilities of failure for all slope angles for the same stability number assumed in Fig. 11.

A comparison between the Figs. 11, 12 and 8 shows that the smaller the value of μ_ϕ (for a constant stability factor), the higher is the effect of the spatial variability of the PS coefficient. In fact, a more nonsmoothed random field with small SOF value of 1.5 m for the PS coefficient will yield a higher probability of failure for lower values of mean friction angle for high slope angles compared to other θ_{Kh} values. This matter is especially important at the occurrence time of earthquakes when the friction angle is so low, thus considering a more non-smoothed random field for the PS coefficient (i.e. a smaller SOF value for that) would be much more effective in such cases.

Finally, it was observed that for a higher mean value for the friction angle (compared to other mean friction values employed for the same constant λ), smaller differences emerge between the resulting probability of failure of each slope regarding different SOF values of the PS coefficient (Fig. 12).

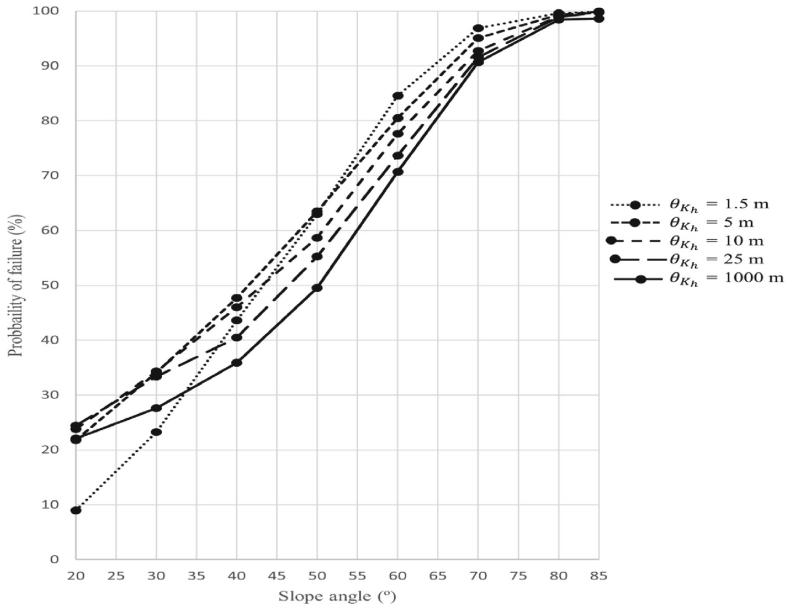

Fig. 8. The influence of θ_{Kh} on probability of slope failure for $\mu_{Kh} = 0.3$, $\mu_\phi = 20^\circ$, $\lambda = 0.4$, $COV_c = 0.3$, $COV_\phi = 0.15$, $COV_{Kh} = 0.5$, $(\theta_{c,\phi})_{Ho}/H = 40$, $(\theta_{c,\phi})_V/H = 0.3$, $\theta_{Kh(H,V)}/H = 0.3$ with a Markovian ACF

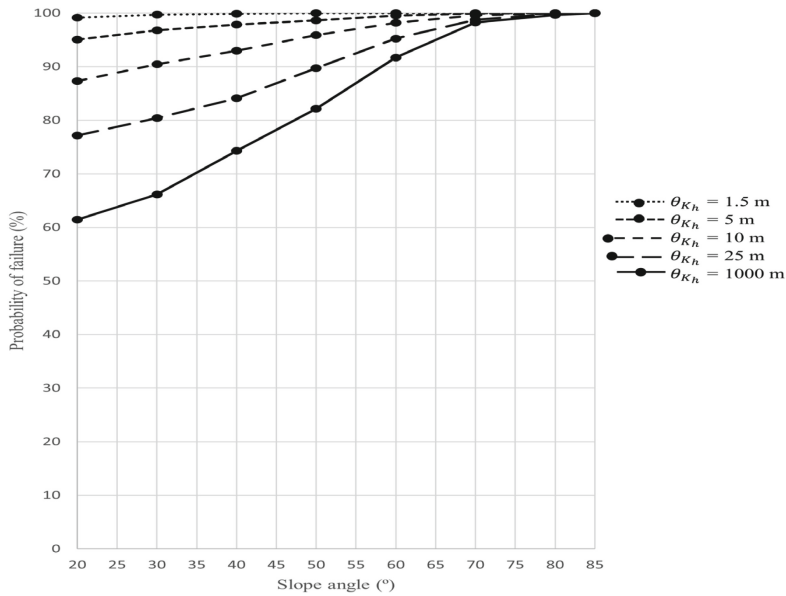

Fig. 9. The influence of θ_{Kh} on probability of slope failure for $\mu_{Kh} = 0.5$, $\mu_\phi = 20^\circ$, $\lambda = 0.4$, $COV_c = 0.3$, $COV_\phi = 0.15$, $COV_{Kh} = 0.5$, $(\theta_{c,\phi})_{Ho}/H = 40$, $(\theta_{c,\phi})_V/H = 0.3$, $\theta_{Kh(H,V)}/H = 0.3$ with a Markovian ACF

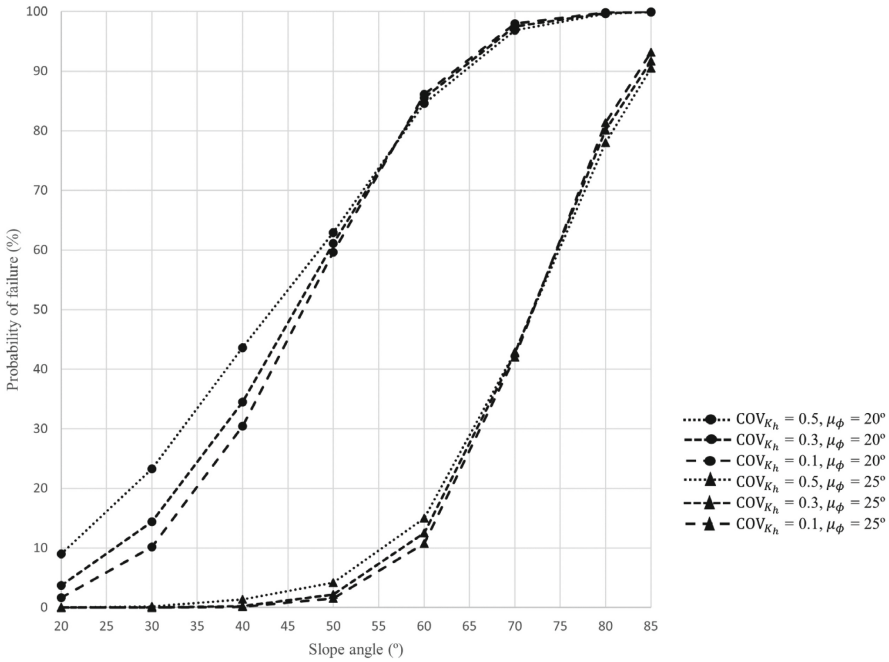

Fig. 10. Influence of mean friction angle on probability of slope failure for $\mu_{Kh} = 0.3$, $\lambda = 0.4$, $\text{COV}_c = 0.3$, $\text{COV}_\phi = 0.15$, $(\theta_{c,\phi})_{Ho}/H = 40$, $(\theta_{c,\phi})_V/H = 0.3$, $\theta_{Kh(H,V)}/H = 0.3$ with a Markovian ACF

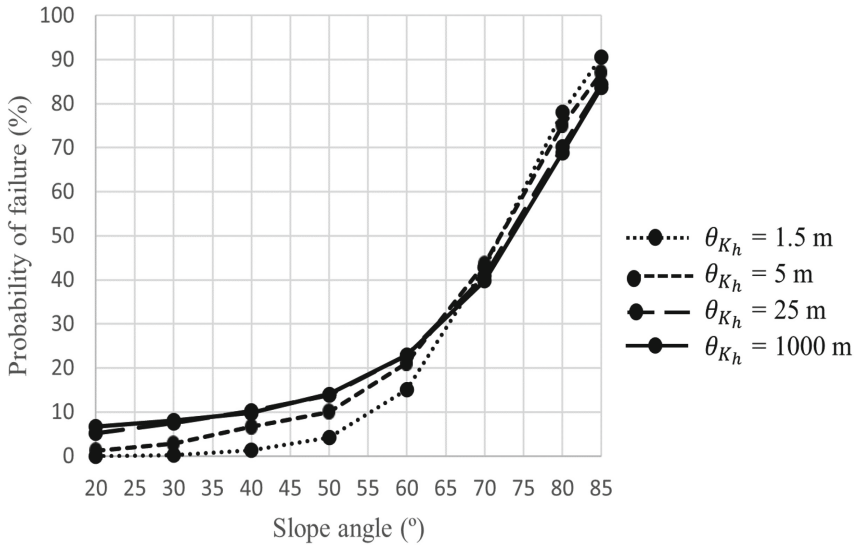

Fig. 11. The influence of θ_{Kh} on probability of slope failure for $\mu_\phi = 25º$, $\lambda = 0.4$, $\mu_{Kh} = 0.3$, $\text{COV}_{Kh} = 0.5$, $\text{COV}_c = 0.3$, $\text{COV}_\phi = 0.15$, $(\theta_{c,\phi})_{Ho}/H = 40$, $(\theta_{c,\phi})_V/H = 0.3$ with a Markovian ACF

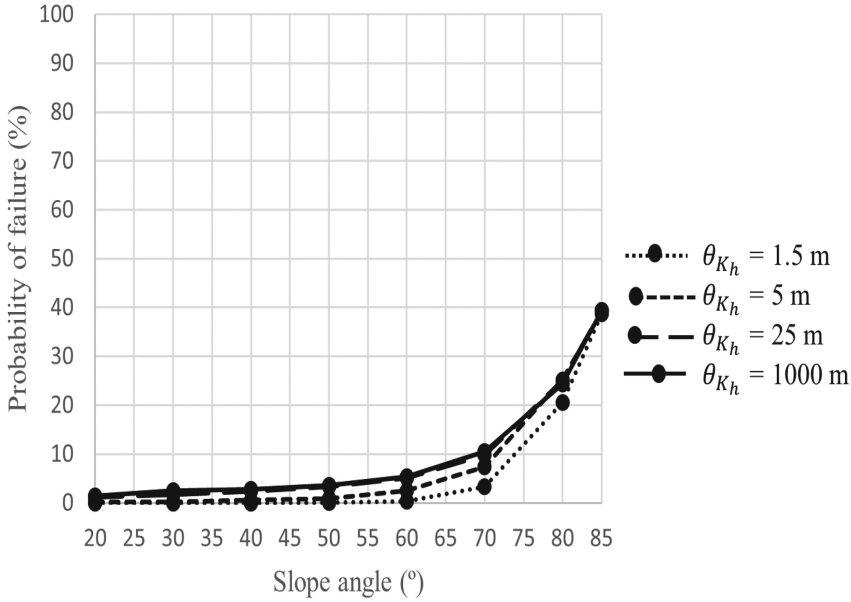

Fig. 12. The influence of θ_{Kh} on probability of slope failure for $\mu_\phi = 30°$, $\lambda = 0.4$, $\mu_{Kh} = 0.3$, $\text{COV}_{Kh} = 0.5$, $\text{COV}_c = 0.3$, $\text{COV}_\phi = 0.15$, $(\theta_{c,\phi})_{Ho}/H = 40$, $(\theta_{c,\phi})_V/H = 0.3$ with a Markovian ACF

5 Conclusion

The current novel methodology considers the simultaneous effect of the soil and PS coefficient spatial variability in the context of probabilistic slope stability analysis using 2D-RLEM approach. Due to the computational efficiency of employing the PS approach compared to a rigorous dynamic one, this novel methodology aligns with sustainable solutions. The underlying conclusions from parametric studies are summarized as follows.

- For small values of PS coefficient, different values of neither COV_{Kh} nor θ_{Kh} make any changes in the resulting probability of failure of soil slope. The higher the mean value of the PS coefficient, the more distinct is the effect of these factors on the resulting slope probabilities of failure. This justifies the importance of current methodology especially for large magnitude earthquakes which hold a higher equivalent PS coefficient value.
- For a mean value of PS coefficient equal to 0.3, the worst-case COV_{Kh} value (corresponding to the highest probability of failure) changes at a turning point from being 0.5 for smaller and 0.1 for the larger slope angles. The position of this turning point is different for different stability numbers. However, a PS coefficient of 0.5 corresponds to a worst-case COV value of 0.5 for most of the conditions.
- The smallest value for the SOF of the PS coefficient corresponds to the worst-case θ_{Kh} values (resulting in the highest probabilities of failure) for all slope angles when the mean value of PS coefficient is high (i.e. 0.5). This shows the importance of modelling

the PS spatial variability for large earthquakes triggering very high slope probabilities of failure.

- A big difference between the probabilities of failure for considering a highly variable field for the PS coefficient (i.e. SOF = 1.5 m) and disregarding this effect was observed for a large earthquake (i.e. $\mu_{Kh} = 0.5$) for gentle slopes.
- The smaller the mean value for the friction angle, the more critical is the effect of modelling a more non-smoothed random field for the PS coefficient for steep slopes (leading to higher probabilities of failure). Totally, the effect of small SOF values for PS coefficient (i.e. 1.5 m compared to other SOF values) is significant for high values of probability of failure.

References

Baker, J., Bradley, B., Stafford, P.: Spatially distributed systems. In Seismic hazard and risk analysis (pp. 447–482). Cambridge University Press, Cambridge (2021). doi: https://doi.org/10.1017/9781108425056.015

Baker, R., Shukha, R., Operstein, V., Frydman, S.: Stability charts for pseudo-static slope stability analysis. Soil Dyn Earthq Eng 26(9), 813–823 (2006). doi:https://doi.org/10.1016/j.soildyn.2006.01.023

Burgess, J., Fenton, G. A., Griffiths, D. V.: Probabilistic seismic slope stability analysis and design. Can Geotech J 56(12), 1979–1998 (2019). doi: https://doi.org/10.1139/cgj-2017-0544

Cami, B., Javankhoshdel, S., Lam, J., Bathurst, R. J., Yacoub, T.: Probabilistic analysis of a tailings dam using 2D composite circular and non-circular deterministic analysis, SRV approach, and RLEM. In: 70th Canadian Geotechnical Conference, 7 p. Ottawa, Canada (2017).

Cami, B., Javankhoshdel, S., Phoon, K. K., Ching, J.: Scale of fluctuation for spatially varying soils: Estimation methods and values. ASCE-ASME J Risk Uncertain Eng Syst A: Civ Eng 6(4), 03120002 (2020). doi:https://doi.org/10.1061/ajrua6.0001083

Cherubini, C.: Reliability evaluation of shallow foundation bearing capacity on c′, φ′ soils. Can Geotech J 37(1), 264–269 (2000). doi:10.1139/ /t99-096

Choudhury, D., Basu, S., Bray, J. D.: Behaviour of slopes under static and seismic conditions by limit equilibrium method. In: Geo-Denver 2007. Denver, USA (2007). doi: https://doi.org/10.1061/40905(224)6

Duncan, J. M.: Factors of safety and reliability in geotechnical engineering. J Geotech Geoenviron Eng 126(4), 307–316 (2000). doi: https://doi.org/10.1061/(ASCE)1090-0241(2000)126:4(307)

Elkateb, T., Chalaturnyk, R., Robertson, P. K.: An overview of soil heterogeneity: Quantification and implications on geotechnical field problems. Can Geotech J 40(1), 1–15 (2003). doi: https://doi.org/10.1139/t02-090

El-Ramly, H.: Probabilistic analyses of landslide hazards and risks: bridging theory and practice. Ph.D. Thesis. University of Alberta, Edmonton, Alberta (2001).

Fenton, G. A., Griffiths, D. V.: Risk assessment in geotechnical engineering. John Wiley & Sons (2008).

Fenton, G. A., Vanmarcke, E. H.: Simulation of random fields via local average subdivision. J Eng Mech 116(8), 1733–1749 (1990). doi: https://doi.org/10.1061/(ASCE)0733-9399(1990)116:8(1733)

Fredlund, D. G., Krahn, J.: Comparison of slope stability methods of analysis. Can Geotech J 14(3), 429–439 (1977). doi: https://doi.org/10.1139/t77-045

Gazetas, G., Garini, E., Anastasopoulos, I., Georgarakos, T.: Effects of near-fault ground shaking on sliding systems. J Geotech Geoenviron Eng 135(12), 1906–1921 (2009). doi: https://doi.org/10.1061/(ASCE)GT.1943-5606.0000174

Griffiths, D. V., Fenton, G. A.: Probabilistic slope stability analysis by finite elements. J Geotech Geoenviron Eng 130(5), 507–518 (2004). doi: https://doi.org/10.1061/ASCE1090-02412004130:5507

Griffiths, D. V., Huang, J., Fenton, G. A.: Influence of Spatial Variability on Slope Reliability Using 2-D Random Fields. J Geotech Geoenviron Eng 135(10), 1367–1378 (2009). doi: https://doi.org/10.1061/(asce)gt.1943-5606.0000099

Huang, J., Griffiths, D. V.: Determining an appropriate finite element size for modelling the strength of undrained random soils. Comput Geotech 69, 506–513 (2015). doi: https://doi.org/10.1016/j.compgeo.2015.06.020

Huang, J. S., Lyamin, A. V., Griffiths, D. V., Krabbenhoft, K., Sloan, S. W.: Quantitative risk assessment of landslide by limit analysis and random fields. Comput Geotech *53*, 60–67 (2013). doi: https://doi.org/10.1016/j.compgeo.2013.04.009

Huang J. S., Griffiths D. V., Fenton G. A.: System reliability of slopes by RFEM. Soils Found 50(3), 343–353 (2010). doi: https://doi.org/10.3208/sandf.50.343

ISSMGE-TC304 (2021). State-of-the-art review of inherent variability and uncertainty in geotechnical properties and models. International Society of Soil Mechanics and Geotechnical Engineering (ISSMGE) -Technical Committee TC304 'Engineering Practice of Risk Assessment and Management', March 2nd., 2021. Download: http://140.112.12.21/issmge/2021/SOA_Review_on_geotechnical_property_variablity_and_model_uncertainty.pdf

Jamshidi Chenari, R., Alaie, R.: Effects of anisotropy in correlation structure on the stability of an undrained clay slope. Georisk 9(2), 109–123 (2015). doi: https://doi.org/10.1080/17499518.2015.1037844

Javankhoshdel, S., Bathurst, R. J.: Simplified probabilistic slope stability design charts for cohesive and cohesive-frictional (c-ϕ) soils. Can Geotech J 51(9), 1033–1045 (2014). doi: https://doi.org/10.1139/cgj-2013-0385

Javankhoshdel, S., Cami, B., Bathurst, R. J., Corkum, B.: Probabilistic analysis of layered slopes with linearly increasing cohesive strength and 2D spatial variability of soil strength parameters using non-Circular RLEM approach. IFCEE 2018, pp. 133–142 (2018). doi: https://doi.org/10.1061/9780784481585.014

Javankhoshdel, S., Luo, N., Bathurst, R. J.: Probabilistic analysis of simple slopes with cohesive soil strength using RLEM and RFEM. Georisk 11(3), 231–246 (2017). doi: https://doi.org/10.1080/17499518.2016.1235712

Jibson, R. W.: Methods for assessing the stability of slopes during earthquakes- A retrospective. Eng Geol 122(1), 43–50 (2011). doi: https://doi.org/10.1016/j.enggeo.2010.09.017

Koppula, S. D.: Pseudo-static analysis of clay slopes subjected to earthquakes. Géotechnique 34(1), 71–79 (1984).

Leshchinsky, D., San, K.: Pseudostatic seismic stability of slopes: Design charts. J Geotech Eng 120(9):1514–1532 (1994). doi: https://doi.org/10.1061/(ASCE)0733-9410(1994)120:9(1514)

Li, D. Q., Qi, X. H., Phoon, K. K., Zhang, L. M., Zhou, C. B.: Effect of spatially variable shear strength parameters with linearly increasing mean trend on reliability of infinite slopes. Struct Saf 49, 45–55 (2014). doi: https://doi.org/10.1016/j.strusafe.2013.08.005

Loukidis, D., Bandini, P., Salgado, R.: Stability of seismically loaded slopes using limit analysis. Geotechnique 53(5), 463–479 (2003). doi: https://doi.org/10.1680/geot.2003.53.5.463

Melo, C., Sharma, S.: Seismic coefficients for pseudostatic slope analysis. In: 13th World Conference on Earthquake Engineering. Vancouver, Canada (2004).

Michalowski, R. L.: Stability charts for uniform slopes. J Geotech Geoenviron Eng 128(4), 351–355 (2002). doi: https://doi.org/10.1061/ASCE1090-02412002128:4351

Mostyn, G. R., Small, J.: Methods of stability analysis, in Walker, B.F., & Fell, R. (eds.) Soil slope instability and stabilization. Rotterdam: Balkema, pp.71-120. (1987).

Park, S., Kim, W., Lee, J., Baek, Y.: Case study on slope stability changes caused by Earthquakes-Focusing on Gyeongju 5.8 ML EQ. Sustainability (Switzerland) 10(10), 3441 (2018). doi: https://doi.org/10.3390/su10103441

Phoon, K. K., Kulhawy, F. H., Grigoriu, M. D.: Reliability-based design of foundations for transmission line structures. Research project (1995).

Phoon, K. K., Kulhawy, F. H.: Characterization of geotechnical variability. Can Geotech J 36(4), 612–624 (1999a). doi:https://doi.org/10.1139/t99-038

Phoon, K. K., Kulhawy, F. H.: Evaluation of geotechnical property variability. Can Geotech J 36(4), 625-639 (1999b). doi: https://doi.org/10.1139/cgj-36-4-625

Sasanian, S., Soroush, A., Jamshidi Chenari, R.: Effect of transformation uncertainty of soil design parameters on stochastic slope stability evaluations. Arab J Geosci 14(12), (2021). doi: https://doi.org/10.1007/s12517-021-07501-9

Saxena, V., Deodatis, G., Shinozuka, M.: Effect of spatial variation of earthquake ground motion on the nonlinear dynamic response of highway bridges. In: 12th World Conference on Earthquake Engineering, Paper 2227. Auckland, New Zealand (2000).

Shah Malekpoor, P., R. Jamshidi Chenari, S. Javankhoshdel.: Discussion of 'Probabilistic seismic slope stability analysis and design'. Can Geotech J 57 (7), (2020). doi: https://doi.org/10.1139/cgj-2019-0386

Shah Malekpoor, P., Lopez-Querol, S.: A novel stochastic pseudo-static approach for slopes. In: 16th Young Geotechnical Engineers Symposium edited by Stirling, R. and Nadimi, S., Newcastle University (2022). doi: https://doi.org/10.57711/kz8q-q554

Srivastava, A., Babu, G. L. S.: Effect of soil variability on the bearing capacity of clay and in slope stability problems. Eng Geol 108(1), 142–152 (2009). doi: https://doi.org/10.1016/j.enggeo.2009.06.023

Tabarroki, M., Ahmad, F., Banaki, R., Jha, S. K., Ching, J.: Determining the factors of safety of spatially variable slopes modeled by random fields. J Geotech Geoenviron Eng 139(12), 2082–2095 (2013). doi: https://doi.org/10.1061/(asce)gt.1943-5606.0000955

Tsompanakis, Y., Lagaros, N. D., Psarropoulos, P. N., Georgopoulos, E. C.: Probabilistic seismic slope stability assessment of geostructures. Struct Infrastruct Eng 6(1–2), 179–191 (2010). doi: https://doi.org/10.1080/15732470802664001

Vanmarcke, E.: Random fields, analysis and synthesis. MIT Press (1988).

Wu, X. Z.: Trivariate analysis of soil ranking-correlated characteristics and its application to probabilistic stability assessments in geotechnical engineering problems. Soils Found *53*(4), 540–556 (2013). doi: https://doi.org/10.1016/j.sandf.2013.06.006

Youssef Abdel Massih, D., Soubra, A. H., Low, B. K.: Reliability-based analysis and design of strip footings against bearing capacity failure. J Geotech Geoenviron Eng 134(7), (2008). doi: https://doi.org/10.1061/ASCE1090-02412008134:7917

Zhang, Y., Zhang, J., Chen, G., Zheng, L., Li, Y.: Effects of vertical seismic force on initiation of the Daguangbao landslide induced by the 2008 Wenchuan earthquake. Soil Dyn Earthq Eng 73, 91–102 (2015). doi: https://doi.org/10.1016/j.soildyn.2014.06.036